

# Dual-Polarized Intelligent Omni-Surfaces for Independent Reflective-Refractive Transmission

Zizhou Zheng

**Abstract**—Intelligent omni-surface (IOS), which are capable of providing service coverage to mobile users (MUs) in a reflective and a refractive manner, has recently attracted widespread attention. However, the performance of traditionally IOS-aid systems is limited by the intimate coupling between the refraction and reflection behavior of IOS elements. In this letter, to overcome this challenge, we introduce the concept of dual-polarized IOS-assisted communication. More precisely, by employing the polarization domain in the design of IOS, full independent refraction and reflection modes can be delivered. We consider a downlink dual-polarized IOS-aided system, while also accounting for the leakage between different polarizations. To maximize the sum rate, we formulate a joint IOS phase shift and BS beamforming problem and proposed an iterative algorithm to solve the non-convex program. Simulation results validate that dual-polarized IOS significantly enhances the performance than the traditional one.

**Index Terms**—Dual-polarized intelligent omni surface, phase shift design.

## I. INTRODUCTION

RECENTLY, reconfigurable intelligent surface (RIS)-assisted wireless communication has attracted great attention, since it enables cost-effective and energy-efficient high data rate communication for future sixth-generation (6G) communication systems. An RIS is an ultra-thin surface containing multiple sub-wavelength nearly passive scattering elements, which is capable of adjusting radio propagation conditions by controlling the phase shifts of the signals that impinge on the surface. Intelligent omni-surface (IOS) is an important instance of an RIS. It can provide service coverage to users on both sides of the surface and overcomes the limitation of widely studied RISs, which only serve users on one side of the surface.

An IOS significantly extends the service coverage of the BS when compared to the traditional RIS and shows great potential for 6G communication [1]. In [2], the authors consider a jointly digital and analog beamforming at the base station (BS) and IOS, respectively. In [3], multiple indoor users obtain omni-directionally services from a small base station with the aid of an IOS. In these studies, the power ratio of the reflected and refracted signals is dependent on the structure of each IOS element and cannot be altered once designed [4], [5], [6]. Therefore, when the ratio of users on both sides is unbalanced with the power ratio, the performance of the IOS-assisted communication system is poor. Additionally, the

Z. Zheng is with the School of Electronics, Peking University, Beijing 100871, China, and also with School of Information Science and Engineering, Southeast University, Nanjing, China (e-mail: 213211229@seu.edu.cn).

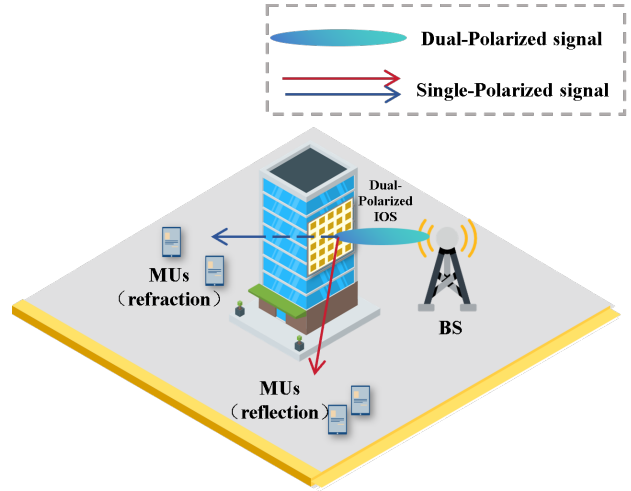


Fig. 1. System model for a dual-polarized IOS-aided MISO downlink system.

optimal deployment position of the IOS also depends on the fixed power ration [7].

To address this issue and realize the full potential of reconfigurable IOS-aided systems, the concept of dual-polarized IOS is proposed [8]. By utilizing the polarization domain, fully independent refraction and reflection modes can be delivered. The polarized IOS element can treat vertical and horizontal polarizations with different polarization-independent electromagnetic response. Then, the power ratio of the refraction and reflection can be equivalently altered by allocating power to different polarized antennas at the BS.

Inspired by this, in this letter, we consider a downlink dual-polarized IOS-assisted system, while also accounting for the leakage between different polarizations. The main contributions are summarized as follows:

- We propose a multi-user dual-polarized IOS-assisted downlink communication system. The physical characteristics of the IOS and the polarization leakage of the considered system model are introduced and discussed
- Based on this, we formulate a joint BS digital and IOS analog beamforming problem, and aim to maximize the sum rate of the users on both sides of the IOS.
- We further analyze the impact of the polarization leakage and user ratio on both sides of the IOS on the performance of the dual-polarized IOS-assisted system and compare the system with the traditional IOS-aided one in the simulation.

The rest of this letter is organized as follows. In Section II, we introduce the system model for dual-polarized IOS-

assisted communications and formulated the jointly digital and analog beamforming problem. In Section III, the original problem is reformulated as a more tractable form and divided into several sub-problems. Then, an iterative algorithm is proposed for addressing this problem. The theoretical analysis are elaborated in Section IV. Numerical results in Section V validate the performance enhancement of the dual-polarized IOS. Finally, conclusions are drawn in Section VI.

## II. SYSTEM MODEL AND PROBLEM FORMULATION

### A. Scenario Description

As shown in Fig. 1, we consider a multi-user polarized multiple-input-multiple-output (MISO) network, where one BS of  $N_t$  dual-polarized antennas communicates with  $2K$  mobile users (MUs). Each user is equipped with an *reconfigurable* antenna, which allows to select one of the polarizations for receiving signals [8]. The dual-polarized intelligent omni-surface (IOS) with  $M$  polarized elements is deployed between the BS and users to reflect or refract the transmit signal. It can choose one polarization for reflection and the other one for refraction. The MUs are divided into two subsets according to their location with respect to the IOS. The subset receiving the reflected signal from the IOS is denoted by  $\mathcal{N}_r$ , and the other subset is denoted by  $\mathcal{N}_t$ , with  $\mathcal{N}_r \cup \mathcal{N}_t = 2K$ .

### B. System Model

The signal transmitted from the BS is expressed as

$$\mathbf{x} = [\mathbf{W}_r, \mathbf{W}_t] \mathbf{s} = \begin{bmatrix} \mathbf{x}_v \\ \mathbf{x}_h \end{bmatrix} \in \mathbb{C}^{2N_t \times 1}, \quad (1)$$

where  $\mathbf{s} \sim \mathcal{CN}(0, \mathbf{I}) \in \mathbb{C}^{2K \times 1}$  denotes different data streams for the MUs,  $\mathbf{W} = [\mathbf{W}_r, \mathbf{W}_t]$  denotes the beamforming matrix, and  $\mathbf{x}_v, \mathbf{x}_h$  represents the signal transmitted from the vertically and horizontally polarized antennas, respectively.

1) *Polarized IOS*: The electromagnetic (EM) response  $g_m$  of the  $m^{\text{th}}$  IOS element takes different values depending on the signal's polarization state and are shown as follows.

$$g_m^{\mathcal{X}} = \begin{cases} g_m^{vv}, & \text{vertically polarized,} \\ g_m^{hh}, & \text{horizontally polarized.} \end{cases} \quad (2)$$

where we define  $\mathcal{X} \in \{vv, hh\}$  as an indicator.

The EM response of the  $m^{\text{th}}$  dual-polarized IOS element to the incident signal, i.e.,  $g_m$ , is an angle-dependent value and can be modeled as

$$g_m^{\mathcal{X}} = \sqrt{G_m F_m (\theta_{i,m}^{\mathcal{X}}, \phi_{i,m}^{\mathcal{X}}) F_m (\theta_{r,m}^{\mathcal{X}}, \phi_{r,m}^{\mathcal{X}}) S_m e^{j\psi_m^{\mathcal{X}}}}, \quad (3)$$

where  $G_m$  is the power gain,  $S_m$  is the surface area of the IOS element and  $F_m$  is the normalized radiation intensity of the IOS element in different directions.  $(\theta_{i,m}^{\mathcal{X}}, \phi_{i,m}^{\mathcal{X}})$  is the incident angle from the transmitting antenna to the  $m^{\text{th}}$  element,  $(\theta_{r,m}^{\mathcal{X}}, \phi_{r,m}^{\mathcal{X}})$  is the departure angle from the  $m^{\text{th}}$  element to the receiving antenna, and  $\psi_m^{\mathcal{X}}$  are the phase shift adjustments that are imposed on the signal.

We assume that the polarized IOS is equipped with  $N$ -bits elements. Then, the available phase shift set is denoted by  $\mathcal{S}_a = \{0, \dots, \frac{2\pi}{2^N} (2^N - 1)\}$  and the phase shift of the  $m^{\text{th}}$  element  $\psi_m \in \mathcal{S}_a$ .

It is noted that for dual-polarized IOS, the phase adjustments of the refracted and reflected link can be independently controlled due to the use of the polarization domain in the design and operation of IOS, while for conventional IOS, the refraction and reflection coefficients are intimately coupled due to the electromagnetic properties of the surface [9].

2) *Channel Model*: In ideal situation, the electromagnetic (EM) waves in orthogonal polarizations exhibit nearly independent propagation characteristics. However, the scatterers in the environment can cause a cross-polarization effect that alters the polarization state of the EM waves and produces polarization leakage. To describe this leakage, we introduce the cross-polarization discrimination (XPD).

Take the channel between the BS and the IOS as an example, which is denoted by

$$\mathbf{H}_{\text{BI}} = \begin{bmatrix} \mathbf{H}_{\text{BI}}^{vv} & \mathbf{H}_{\text{BI}}^{vh} \\ \mathbf{H}_{\text{BI}}^{hv} & \mathbf{H}_{\text{BI}}^{hh} \end{bmatrix} \in \mathbb{C}^{2M \times 2N_t}, \quad (4)$$

where  $\mathbf{H}_{\text{BI}}^{vv}$  and  $\mathbf{H}_{\text{BI}}^{hh}$  are the co-polarized components and  $\mathbf{H}_{\text{BI}}^{vh}$  and  $\mathbf{H}_{\text{BI}}^{hv}$  are the cross-polarized components. The XPD of  $\mathbf{H}_{\text{BI}}$  can be expressed as

$$\text{XPD} = \frac{\mathbb{E}\{\|\mathbf{H}_{\text{BI}}^{vv}\|_F^2\}}{\mathbb{E}\{\|\mathbf{H}_{\text{BI}}^{hv}\|_F^2\}} = \frac{\mathbb{E}\{\|\mathbf{H}_{\text{BI}}^{hh}\|_F^2\}}{\mathbb{E}\{\|\mathbf{H}_{\text{BI}}^{vh}\|_F^2\}} = \frac{1 - \beta_{\text{BI}}}{\beta_{\text{BI}}}, \quad (5)$$

where  $\beta_{\text{BI}}$  is the XPD factor.

The channel  $\mathbf{h}_{\text{IU},k}$  between the IOS and the  $k^{\text{th}}$  user is defined as

$$\mathbf{h}_{\text{IU},k} = \begin{cases} [\mathbf{h}_{\text{IU},k}^{vv}, \mathbf{h}_{\text{IU},k}^{vh}], & k \in \mathcal{N}_r \\ [\mathbf{h}_{\text{IU},k}^{hv}, \mathbf{h}_{\text{IU},k}^{hh}], & k \in \mathcal{N}_t, \end{cases} \quad (6)$$

where the channel XPD factor is defined as  $\beta_{\text{IU},k}$ . The direct path  $\mathbf{h}_{\text{BU},k}$  between the BS and the  $k^{\text{th}}$  MU can be similarly modeled.

### C. IOS-based Beamforming

The received signal at the  $k^{\text{th}}$  MU is expressed as

$$y_k = (\mathbf{h}_{\text{BU},k} + \mathbf{h}_{\text{IU},k} \mathbf{G} \mathbf{H}_{\text{BI}}) \mathbf{x} + n_k \\ = \mathbf{h}_k \mathbf{x} + n_k, \quad (7)$$

where the IOS coefficient matrix  $\mathbf{G}$  is denoted by  $\text{diag}\{g_1^{vv}, \dots, g_m^{vv}, g_1^{hh}, \dots, g_m^{hh}\}$ ,  $\mathbf{h}_k = \mathbf{h}_{\text{BU},k} + \mathbf{h}_{\text{IU},k} \mathbf{G} \mathbf{H}_{\text{BI}}$  represents the equivalent channel between the BS and the  $k^{\text{th}}$  user, and  $n_k$  is the additive white Gaussian noise (AWGN) at the  $k^{\text{th}}$  user whose mean is zero and variance is  $\sigma^2$ .

Assume that the channel state information (CSI) is known at the transmitter. Based on the received signal in (7), the signal-to-interference-plus-noise ratio (SINR) of the  $k^{\text{th}}$  MU in the reflected side can be formulated as

$$\gamma_{k_r} = \frac{|\mathbf{h}_{r,k_r} \mathbf{W}_r^{(k_r)}|^2}{\sum_{k'_r \neq k_r} |\mathbf{h}_{r,k_r} \mathbf{W}_r^{(k'_r)}|^2 + \sum_{i \in \mathcal{N}_t} |\mathbf{h}_{r,k_r} \mathbf{W}_t^{(i)}|^2 + \sigma^2}, \quad (8)$$

where  $\mathbf{W}^{(k)}$  denotes the  $k^{\text{th}}$  column of the beamformer  $\mathbf{W}$ ,  $\sum_{k'_r \neq k_r} |\mathbf{h}_{r,k_r} \mathbf{W}_r^{(k'_r)}|^2$  denotes the interference of MUs with same polarization, and  $\sum_{i \in \mathcal{N}_t} |\mathbf{h}_{r,k_r} \mathbf{W}_t^{(i)}|^2$  represents the polarization leakage of other MUs with different polarization. The SINRs of the users equipped with a horizontally polarized antenna can be similarly written.

### D. Problem formulation

The optimization problem can be formulated as

$$\max_{\substack{\mathbf{W}_r, \mathbf{W}_t \\ \{\psi_m^{vv}\}, \{\psi_m^{hh}\}}} \sum_{k_r \in \mathcal{N}_r} \log_2(1 + \gamma_{k_r}) + \sum_{k_t \in \mathcal{N}_t} \log_2(1 + \gamma_{k_t}) \quad (9a)$$

$$\text{s.t.} \quad \text{Tr}(\mathbf{W}_r \mathbf{W}_r^H) + \text{Tr}(\mathbf{W}_t \mathbf{W}_t^H) \leq P_{\text{BS}}, \quad (9b)$$

$$\psi_m^{\mathcal{X}} \in \mathcal{S}_a, \quad (9c)$$

where  $P_{\text{BS}}$  denotes the maximum transmit power at the BS.

### III. DUAL-POLARIZED IOS-BASED BEAMFORMING ALGORITHM

In this section, we first transform (9) into a more tractable one, which decouples the optimization of the digital and analog beamforming at the BS and the IOS, respectively. Then, the original problem can be separated into several sub-problems.

#### A. Reformulate of the original problem

The minimum mean-square error (MMSE) algorithm is employed for addressing the non-convex (9a). By introducing the auxiliary variables  $\mathbf{f} = [f_{r,1}, \dots, f_{r,N_r}, f_{t,1}, \dots, f_{t,N_t}]^T$ , and  $\mathbf{u} = [u_{r,1}, \dots, u_{r,N_r}, u_{t,1}, \dots, u_{t,N_t}]^T$ , Problem (9) can be reformulated as

$$\max_{\substack{\mathbf{W}_r, \mathbf{W}_t \\ \mathbf{G}, \mathbf{f}, \mathbf{u}}} \sum_{k_r \in \mathcal{N}_r} (\log_2 f_{r,k_r} - f_{r,k_r} e_{r,k_r}) + \sum_{k_t \in \mathcal{N}_t} (\log_2 f_{t,k_t} - f_{t,k_t} e_{t,k_t}) \quad (10a)$$

$$\text{s.t.} \quad (9b), (9c), \quad (10b)$$

where the MSE of the  $k_r$ <sup>th</sup> MU receiving the reflected signal is given by

$$\begin{aligned} e_{r,k_r} &= \mathbb{E} \left\{ \left( u_{r,k_r}^* y_{r,k_r} - s_{r,k_r} \right) \left( u_{r,k_r}^* y_{r,k_r} - s_{r,k_r} \right)^* \right\} \\ &= \sum_{i \in \mathcal{K}_r} \left| u_{r,k_r}^* \mathbf{h}_{r,k_r} \mathbf{W}_r^{(i)} \right|^2 + \sum_{j \in \mathcal{K}_t} \left| u_{r,k_r}^* \mathbf{h}_{r,k_r} \mathbf{W}_t^{(j)} \right|^2 \\ &\quad - 2 \text{Re} \left\{ u_{r,k_r}^* \mathbf{h}_{r,k_r} \mathbf{W}_r^{(k_r)} \right\} + |u_{r,k_r}|^2 \sigma^2 + 1. \end{aligned} \quad (11)$$

By taking the first derivative of (10a) and (11) equal to zero, we obtain the optimal solutions of  $f_{r,k_r}$  and  $u_{r,k_r}$  as

$$u_{r,k_r}^* = \frac{\mathbf{h}_{r,k_r} \mathbf{W}_r^{(k_r)}}{\|\mathbf{h}_{r,k_r} [\mathbf{W}_r, \mathbf{W}_t]\|^2 + \sigma^2}, \quad (12)$$

$$f_{r,k_r}^* = \frac{1}{1 - u_{r,k_r}^{op} \mathbf{W}_r^{(k_r)H} \mathbf{h}_{r,k_r}^H}. \quad (13)$$

In the following, we focus on the optimization of the digital and analog beamformer  $\mathbf{W}_r, \mathbf{W}_t$  and  $\mathbf{G}$ .

#### B. Digital beamforming optimization at the BS

With fixed  $\mathbf{f}$ ,  $\mathbf{u}$ , and  $\mathbf{G}$ , Problem (10) is rewritten as

$$\begin{aligned} \min_{\mathbf{W}_r, \mathbf{W}_t} & \sum_{k_r \in \mathcal{N}_r} f_{r,k_r} (\|u_{r,k_r}^* \mathbf{h}_{r,k_r} \mathbf{W}_r\|^2 - 2 \text{Re}\{u_{r,k_r}^* \mathbf{h}_{r,k_r} \mathbf{W}_r^{(k_r)}\}) \\ & + \sum_{k_t \in \mathcal{N}_t} f_{t,k_t} (\|u_{t,k_t}^* \mathbf{h}_{t,k_t} \mathbf{W}_t\|^2 - 2 \text{Re}\{u_{t,k_t}^* \mathbf{h}_{t,k_t} \mathbf{W}_t^{(k_t)}\}) \end{aligned} \quad (14a)$$

$$\text{s.t.} \quad \text{Tr}(\mathbf{W}_r \mathbf{W}_r^H) + \text{Tr}(\mathbf{W}_t \mathbf{W}_t^H) \leq P_{\text{BS}}. \quad (14b)$$

The Lagrangian function of Problem (14) is written as

$$\begin{aligned} \mathcal{L}(\mathbf{W}_r, \mathbf{W}_t, \lambda) &= \lambda \left( \sum_{i \in \mathcal{N}_r} \mathbf{W}_r^{(i)H} \mathbf{W}_r^{(i)} + \sum_{j \in \mathcal{N}_t} \mathbf{W}_t^{(j)H} \mathbf{W}_t^{(j)} \right) \\ &\quad - \sum_{i \in \mathcal{N}_r} 2f_{r,i} \text{Re}\{u_{r,i}^* \mathbf{h}_{r,i} \mathbf{W}_r^{(i)}\} - \sum_{j \in \mathcal{N}_t} 2f_{t,j} \text{Re}\{u_{t,j}^* \mathbf{h}_{t,j} \mathbf{W}_t^{(j)}\} \\ &\quad + \sum_{i \in \mathcal{N}_r} \mathbf{W}_r^{(i)H} \mathbf{M} \mathbf{W}_r^{(i)} + \sum_{j \in \mathcal{N}_t} \mathbf{W}_t^{(j)H} \mathbf{M} \mathbf{W}_t^{(j)} - \lambda P_{\text{BS}}, \end{aligned} \quad (15)$$

where  $\mathbf{M} = \sum f_{r,i} |u_{r,i}|^2 \mathbf{h}_{r,i}^H \mathbf{h}_{r,i} + \sum f_{t,j} |u_{t,j}|^2 \mathbf{h}_{t,j}^H \mathbf{h}_{t,j}$ , and  $\lambda \geq 0$  is the Lagrangian multiplier with the constraint (9b).

By setting the first-order derivative of  $\mathcal{L}(\mathbf{W}_r, \mathbf{W}_t, \lambda)$  w.r.t.  $\mathbf{W}_r^{(k_r)}, \mathbf{W}_t^{(k_t)}$  to zero, the optimal solution is given by

$$\mathbf{W}_r^{(k_r)*}(\lambda) = u_{r,k_r} f_{r,k_r} (\mathbf{M} + \lambda \mathbf{I})^\dagger \mathbf{h}_{r,k_r}^H, \quad (16)$$

$$\mathbf{W}_t^{(k_t)*}(\lambda) = u_{t,k_t} f_{t,k_t} (\mathbf{M} + \lambda \mathbf{I})^\dagger \mathbf{h}_{t,k_t}^H, \quad (17)$$

where  $(\cdot)^\dagger$  denotes the matrix pseudo-inverse. The value of  $\lambda$  should satisfy the complementary slackness condition  $\lambda (\sum_{i \in \mathcal{N}_r} \mathbf{W}_r^{(i)H} \mathbf{W}_r^{(i)} + \sum_{j \in \mathcal{N}_t} \mathbf{W}_t^{(j)H} \mathbf{W}_t^{(j)} - P_{\text{BS}}) = 0$ . The value of  $\lambda$  should be chosen for ensuring the following equation:

$$\mathcal{F}(\lambda) \triangleq \sum_{i=1}^{2N_t} \frac{\left[ \sum_{k=1}^{2K} |u_k f_k|^2 \mathbf{Q}^H \mathbf{h}_k^H \mathbf{h}_k \mathbf{Q} \right]_{i,i}}{([\mathbf{\Lambda}]_{i,i} + \lambda)^2} = P_{\text{BS}}. \quad (18)$$

where  $[\cdot]_{i,i}$  denotes the  $i$ th diagonal element of the matrix. The unitary matrix  $\mathbf{Q}$  and the diagonal matrix  $\mathbf{\Lambda}$  are derived from the singular value decomposition (SVD) of the matrix  $\mathbf{M} = \mathbf{Q} \mathbf{\Lambda} \mathbf{Q}^H$ , where  $\mathbf{Q} \mathbf{Q}^H = \mathbf{Q}^H \mathbf{Q} = \mathbf{I}_{2N_t}$ .

Readily, the total power consumption  $\mathcal{F}(\lambda)$  is a decreasing function of  $\lambda$  and  $\mathcal{F}(\infty) = 0$ . Thus, the bisection search method can be employed to find  $\lambda$ , and the upper bound of  $\lambda$  is given by  $\lambda \leq \sqrt{\frac{\sum_{i=1}^{2N_t} [\sum_{k=1}^{2K} |u_k f_k|^2 \mathbf{Q}^H \mathbf{h}_k^H \mathbf{h}_k \mathbf{Q}]_{i,i}}{P_{\text{BS}}}} = \lambda^{ub}$ .

#### C. Analog beamforming optimization at the IOS

Given the optimal  $\mathbf{f}$ ,  $\mathbf{u}$ ,  $\mathbf{W}_r$ , and  $\mathbf{W}_t$ , the discrete analog beamforming subproblem can be written as

$$\min_{\mathbf{G}} \quad \text{Tr}(\mathbf{G}^H \mathbf{B} \mathbf{G} \mathbf{C}) + 2 \text{Re}\{\text{Tr}(\mathbf{G} \mathbf{V})\} \quad (19a)$$

$$\text{s.t.} \quad (9c), \quad (19b)$$

where  $\mathbf{B} = \sum_{k_r \in \mathcal{N}_r} f_{r,k_r} u_{r,k_r} u_{r,k_r}^* \mathbf{h}_{\text{IU},k_r}^H \mathbf{h}_{\text{IU},k_r} + \sum_{k_t \in \mathcal{N}_t} f_{t,k_t} u_{t,k_t} u_{t,k_t}^* \mathbf{h}_{\text{IU},k_t}^H \mathbf{h}_{\text{IU},k_t}$ ,  $\mathbf{C} = \mathbf{H}_{\text{BI}} \mathbf{W} \mathbf{W}^H \mathbf{H}_{\text{BI}}^H$ , and  $\mathbf{V} = \sum_{i \in \mathcal{N}_r} f_{r,i} u_{r,i}^* (u_{r,i} \mathbf{H}_{\text{BI}} \mathbf{W} \mathbf{W}^H \mathbf{h}_{\text{BU},i}^H \mathbf{h}_{\text{IU},i} - \mathbf{H}_{\text{BI}} \mathbf{W}_r^{(i)} \mathbf{h}_{\text{IU},i}) + \sum_{j \in \mathcal{N}_t} f_{t,j} u_{t,j}^* (u_{t,j} \mathbf{H}_{\text{BI}} \mathbf{W} \mathbf{W}^H \mathbf{h}_{\text{BU},j}^H \mathbf{h}_{\text{IU},j} - \mathbf{H}_{\text{BI}} \mathbf{W}_t^{(j)} \mathbf{h}_{\text{IU},j})$ .

Problem (19) is tackled in two steps: (i) we first consider a relaxed problem with continuous phase shifts and (ii) then a branch-and-bound based algorithm is proposed to account for the discrete phase shifts.

The objective function in (19) is a convex function of the IOS coefficient matrix  $\mathbf{G}$ . By releasing the non-convex (9c), it can be solved by standard tools such as CVX.

However,  $\psi_m^{X,opt}$  lies in the range of  $l_m \Delta\psi$  and  $(l_m + 1) \Delta\psi$ , where  $l_m$  denotes an integer satisfying  $0 \leq l_m \Delta\psi \leq \frac{2\pi}{2^N} (2^N - 1)$ , and  $\Delta\psi = \frac{2\pi}{2^N}$  represents the discrete phase shift step, which can be addressed by branch-and-bound (BnB) algorithm [3].

#### D. Overall Algorithm

Based on the above analysis, we provide the detailed steps of the algorithm to solve Problem (9) in Algorithm 1.

---

#### Algorithm 1 Joint Digital and Analog Beamforming design for Sum-Rate Maximization Problem

---

- 1: Initialize  $\mathbf{W}_r, \mathbf{W}_t, \{\psi_m^{vv}\}, \{\psi_m^{hh}\}$ .
  - 2: **While** no convergence of the objective function (10a)
  - 3:   Update  $\mathbf{f}$  by (12);
  - 4:   Update  $\mathbf{u}$  by (13);
  - 5:   Calculate the  $\lambda$  by adopting bisection search method in  $[0, \lambda^{ub})$  based on (18);
  - 6:   Update  $\mathbf{W}_r$  and  $\mathbf{W}_t$  by (16)-(17);
  - 7:   Update  $\mathbf{G}$  by solving Problem (19) relaxing (9c);
  - 8:   Calculate the optimal  $\mathbf{G}$  with discrete phase shift by adopting BnB algorithm;
  - 9: **Until** the objective function (10a) converges.
- 

#### IV. PERFORMANCE ANALYSIS OF THE IOS-ASSISTED COMMUNICATION SYSTEM

In this section, we first discuss the impact of the XPD on the system performance, and then analyze the downlink sum rate as a function of the ratio of the MUs.

##### A. Analysis of the XPD

Given the optimal power allocation based on (16) and (17), we first analyze the impact of polarization leakage, i.e., XPD on the digital beamformer  $\mathbf{W} = [\mathbf{W}_r, \mathbf{W}_t]$ .

*Proposition 1:* If the polarization leakage is zero, each MU's digital beamformer  $\mathbf{W}^{(k)}$  will have half of its elements corresponding to encoding elements in the opposite polarization direction, with values equal to zero.

*Proof:* When there is no polarization leakage, the channel's cross-polarization component does not exist. From the expressions in (16) and (17), it is evident that the conclusion holds.

Then, we discuss the impact of the XPD on the sum rate.

*Proposition 2:* As the cross-polarization factor  $\beta_{\text{BI}}$  given in (5) increases from 0 to 1, the system performance first degrades and then becomes better.

*Proof:* Note that when  $\beta_{\text{BI}} = 0$ , the polarization of the transmitted signal will not change when it propagates from the BS. Alternatively,  $\beta_{\text{BI}} = 1$  correspond to the case that the transmitted signal will be completely converted to the opposite

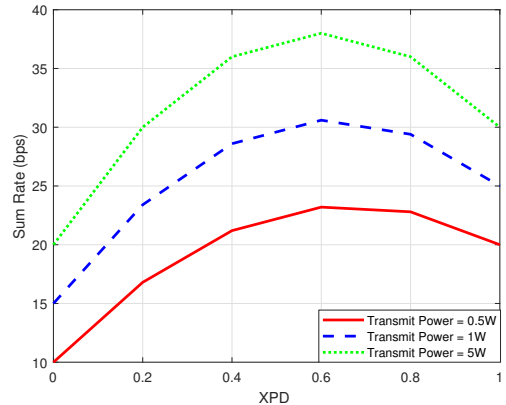


Fig. 2. Sum rate versus XPD with different transmit power.

polarization and can also be decomposed as two dependent subchannels. On the other hand, if  $0 < \beta_{\text{BI}} < 1$ , a part of the power will be leaked to the other polarization, which cause cross-polarization interference and degrade the performance.

Based on *Proposition 2*, we can obtain *Proposition 3*.

*Proposition 3:* Low polarization leakage is not always better for the dual-polarized IOS-assisted systems. High leakage is beneficial for a low transmit power.

*Proof:* The system performance initially decreases and then increases as  $\beta_{\text{BI}}$  increases. In some cases, the worst performance may occur at a smaller value of  $\beta_{\text{BI}}$ , which implies that a larger  $\beta_{\text{BI}}$  could potentially help improve performance.

##### B. Analysis of the user ratio $\mathcal{N}_r/\mathcal{N}_t$

In this section, we analyze the impact of the user ratio of the reflection and refraction on the sum-rate of an IOS-assisted communication system.

*Proposition 4:* Different from traditional IOS, the sum rate of dual-polarized IOS-assisted systems are not impacted by the user ratio  $\mathcal{N}_r/\mathcal{N}_t$ .

*Proof:* The sum rate of traditional IOS-assisted systems is impacted by  $\mathcal{N}_r/\mathcal{N}_t$ , since the elements have a fixed power ratio. When the power ratio is unmatched with the user ratio on both sides, the performance is poor. A dual-polarized IOS-assisted system can overcome this by power allocation for different polarized antennas at the BS. Thus, the sum rate is not impacted by the ratio  $\mathcal{N}_r/\mathcal{N}_t$ .

#### V. SIMULATION RESULTS

In this section, we evaluate the performance of the considered dual-polarized IOS-assisted system based on the proposed algorithm and compare it with an RIS-aided system, a traditional IOS-aided system, and a conventional cellular system in the absence of IRS or IOS. In the conventional cellular system, the MUs receive only the direct links from the BS without the assistance of a reconfigurable surface.

In Figure. 2, we plot the sum rate versus XPD for different transmit power. It can be observed that as the XPD increases from 0 to 1, the communication rate for different transmit powers initially increases and then decreases, which is consistent

with our previous analysis. Furthermore, it is noticeable that the location of the peak is related to the transmit power.

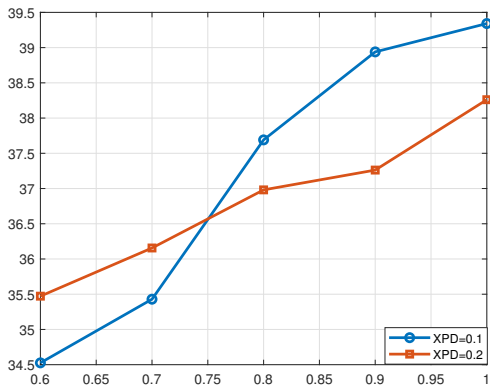


Fig. 3. Sum rate versus transmit power with different XPD.

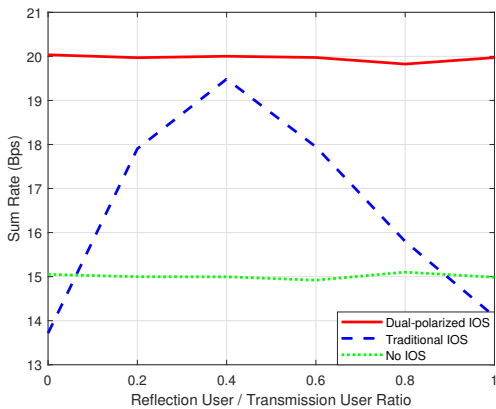


Fig. 4. Sum rate versus transmit power with different user ratio.

In Figure. 3, we plot the sum rate versus the transmit power for different XPD factors. It can be observed that as the transmit power increases, both the system and communication rate improve for the two curves. However, when the XPD factor is 0.1, the communication rate is lower at lower transmit powers, whereas at higher transmit powers, the communication rate is noticeably higher than when the XPD factor is 0.2. This further validates the previous analysis that a lower XPD is not always beneficial.

In Figure. 4, we plot the sum rate versus the ratio of the reflection user and refraction user for different scenarios. We have demonstrated the impact of the user ratio on system performance in MISO communication systems with dual-polarized IOS, traditional IOS, and without any IOS assistance. For the traditional IOS, since the transmission-to-reflection ratio is fixed, the system performs well when the user ratio on both sides aligns well with the transmission-reflection ratio. However, in extreme cases, the performance suffers significantly. In contrast, for the polarization IOS, it can allocate signal power to the two sides of the metasurface via precoding at the base station. As a result, the performance is

better compared to the MISO system without IOS assistance, and the system performance is less sensitive to the user ratio.

## VI. CONCLUSION

In this letter, we considered a dual-polarized IOS-aided MISO downlink system and investigated the joint BS digital and ios analog beamforming design to maximize the sum rate for independent reflective-refractive transmission by utilizing the polarization domain. Then, we analyzed the impact of the XPD and the user ratio on both sides of the dual-polarized IOS on the system performance. We have the following conclusions: 1) Unlike traditional IOS, the performance of the polarization IOS is less affected by the ratio of the number of users on both sides, as the coupling between transmission and reflection coefficients is decoupled. 2) Low polarization is not always better for the dual-polarized IOS-aided system.

## REFERENCES

- [1] Y. Liu, X. Mu, J. Xu, R. Schober, Y. Hao, H. V. Poor, and L. Hanzo, "STAR: Simultaneous transmission and reflection for 360° coverage by intelligent surfaces," *IEEE Wireless Commun.*, vol. 28, no. 6, pp. 102–109, Jan. 2021.
- [2] W. Cai, M. Li, Y. Liu, Q. Wu, and Q. Liu, "Joint beamforming design for intelligent omni surface assisted wireless communication systems," *IEEE Trans. Wireless Commun.*, vol. 22, no. 2, pp. 1281–1297, Sep 2023.
- [3] S. Zhang, H. Zhang, B. Di, Y. Tan, M. Di Renzo, Z. Han, H. Vincent Poor, and L. Song, "Intelligent omni-surfaces: Ubiquitous wireless transmission by reflective-refractive metasurfaces," *IEEE Trans. Wireless Commun.*, vol. 21, no. 1, pp. 219–233, Jul. 2022.
- [4] S. Zeng, H. Zhang, B. Di, Y. Tan, Z. Han, H. V. Poor, and L. Song, "Reconfigurable intelligent surfaces in 6G: Reflective, transmissive, or both?" *IEEE Commun. Lett.*, vol. 25, no. 6, pp. 2063–2067, Feb. 2021.
- [5] M. A. ElMossallamy, H. Zhang, L. Song, K. G. Seddik, Z. Han, and G. Y. Li, "Reconfigurable intelligent surfaces for wireless communications: Principles, challenges, and opportunities," *IEEE Trans. Cogn. Commun. Netw.*, vol. 6, no. 3, pp. 990–1002, May 2020.
- [6] R. Deng, B. Di, H. Zhang, Y. Tan, and L. Song, "Reconfigurable holographic surface-enabled multi-user wireless communications: Amplitude-controlled holographic beamforming," *IEEE Trans. Wireless Commun.*, vol. 21, no. 8, pp. 6003–6017, Jan. 2022.
- [7] M. Li, S. Zeng, H. Zhang, B. Di, X. Weng, and L. Song, "Intelligent omni-surfaces (IOSs) for full-dimensional wireless coverage extension: IOS orientation and location optimization," in *2024 IEEE/CIC Int. Conf. Commun. China (ICCC)*, Sep. 2024, pp. 1027–1032.
- [8] A. Palomares-Caballero, C. Moleró, F. R. Ghadi, F. J. López-Martínez, P. Padilla, D. Morales-Jimenez, and J. F. Valenzuela-Valdés, "Enabling intelligent omni-surfaces in the polarization domain: Principles, implementation and applications," *IEEE Commun. Mag.*, vol. 61, no. 11, pp. 144–150, Nov. 2023.
- [9] J. Xu, Y. Liu, X. Mu, R. Schober, and H. V. Poor, "STAR-RIS: A correlated T&R phase-shift model and practical phase-shift configuration strategies," *IEEE J. Sel. Topics Signal Process.*, vol. 16, no. 5, pp. 1097–1111, May 2022.